Polar Geosci., **14**, 180–194, 2001

Laboratory measurements of *P*-wave velocity of granulites from Lützow-Holm Complex, East Antarctica: Preliminary report

Keigo Kitamura[1], Masahiro Ishikawa[2], Makoto Arima[2] and Kazuyuki Shiraishi[3]

[1]*Department of Polar Science, School of Mathematical and Physical Science, The Graduate University for Advanced Studies, Kaga 1-chome, Itabashi-ku, Tokyo 173-8515*
[2]*Graduate School of Environment and Information Sciences, Yokohama National University, Tokiwadai 79-7, Hodogaya-ku, Yokohama 240-8501*
[3]*National Institute of Polar Research, Kaga 1-chome, Itabashi-ku, Tokyo 173-8515*

Abstract: *P*-wave velocities (*Vp*) were measured for nine samples of granulite facies metamorphic rock from the early Paleozoic Lützow-Holm Complex, East Antarctica. The measurements were done at pressures from 0.1 GPa to 1.0 GPa and at temperatures from 25°C to 400°C with a piston-cylinder apparatus. *Vp* values of the ultrabasic-basic granulites range from 6.65 to 7.29 km/s at 1.0 GPa and 25°C. The felsic gneiss shows nearly constant *Vp* value from 25°C to 400°C at 0.6 and 1.0 GPa, whereas it exhibits rapid decrease of *Vp* with increasing temperature at 0.4 GPa. In all rock samples measured, the biotite-two pyroxene granulite shows the strongest negative thermal effect of *Vp* (0.45 km/s). This strong thermal effect is attributed to relatively higher biotite abundance.

key words: *P*-wave velocity, Lützow-Holm Complex, granulite, biotite

1. Introduction

Assessment of chemical and petrological compositions of a continental crust is essential to understand the processes of formation and evolution of crusts. The chemical composition of the uppermost part of the continental crust has been elucidated by detailed geological and petrological investigations (*e.g.* Condie, 1997). However, it is a difficult task to estimate the chemistry and rock types of the deep continental crust by surface geology. Xenoliths of lower crustal origin and deep coring samples are not always representative of the deep crustal material because the available amounts of these samples are not enough and they are derived from rather small areas. In contrast, granulite facies metamorphic terranes are composed of various kinds of rocks and we can collect samples from wide areas to compare with samples from xenoliths and boring cores.

Seismological studies reveal physical and geometrical characteristics of extensive areas of the continental crust (*e.g.*, Blundell *et al.*, 1992). However, estimation of the rock constitutions of deeper parts of the continental crust is not possible from the seismological data without laboratory measurement of rock velocity. Comparison of the seismological velocity structure of the crust with laboratory data on high-grade

metamorphic rocks is vital for understanding the lithology of the deep continental crust.

The early Paleozoic Lützow-Holm Complex in East Antarctica consists mainly of high-grade metamorphic rocks in which the metamorphic grade increases from amphibolite facies in the east to granulite facies in the southwest over 250 km. The Lützow-Holm Complex has been well characterized geologically and petrologically by the Japanese Antarctic Research Expeditions (JARE), and the Complex is regarded as a part of the Pan-African orogenic belt (Shiraishi *et al.*, 1994). The peak metamorphic conditions at the granulite facies zone are estimated to be 1000°C at 1.1 GPa (Motoyoshi and Ishikawa, 1997).

A seismic experiment was carried out along a route between Syowa Station and Mizuho Station in 1980–1981 to elucidate the velocity structure beneath the Mizuho Plateau (Fig. 1). *P*-wave arrival time data suggest a thin lower crust 10 km thick and Mohorovicic discontinuity at 40 km depth (Ikami *et al.*, 1984). In order to clarify more details of the seismic structures, JARE performed a high-resolution seismic experiment along the same route in 1999–2000 (Miyamachi *et al.*, 2001), and a third experiment crossing the route of 1999–2000 will be performed in 2001–2002. These seismic surveys will be used for modeling 3-dimensinal *P*-wave velocity structures of the Lützow-Holm Complex, essential for understanding the evolution of East Antarctica and formation of the Gondowana super continent (Fig. 1).

In this study, we measured rock *P*-wave velocities of nine granulite samples collected from the Lützow-Holm Complex and discuss pressure and temperature effects on *Vp*, the relationships between *Vp* and rock composition, and *Vp* and mineral assemblage.

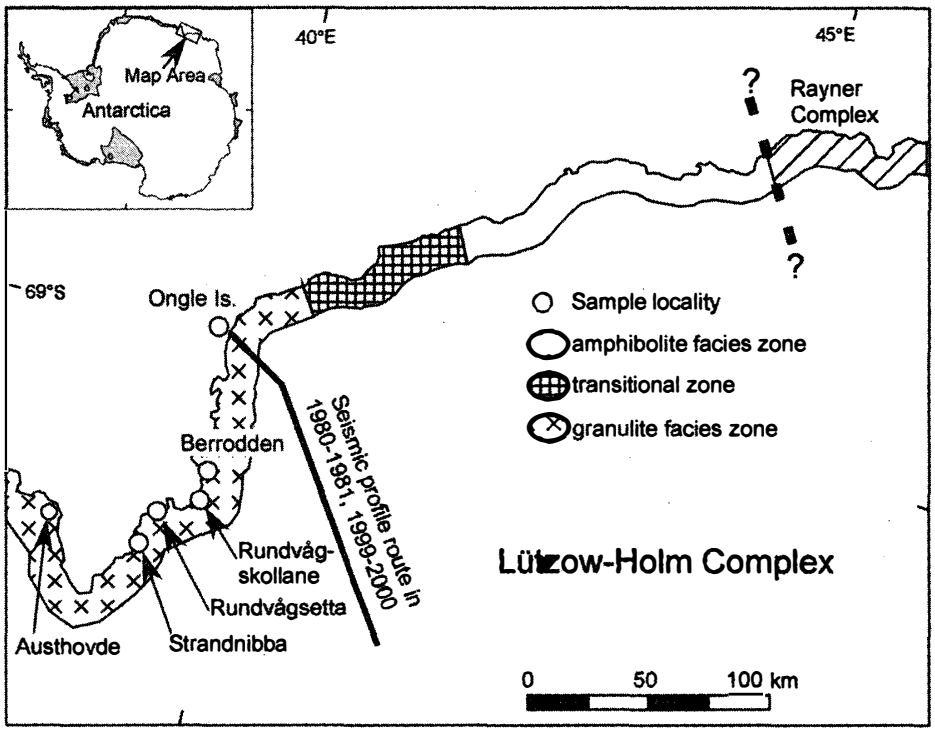

Fig. 1. Metamorphic facies map of Lützow-Holm Complex with isograde in rocks of various compositions (modified after Hiroi et al., 1991).

2. Sample descriptions

The rock samples measured were selected from the rock collection of the National Institute of Polar Research (NIPR). These samples have a wide range of SiO_2 content from ultra-basic to acidic composition (44.8–81.3 wt%) (Table 1). Major and trace elements were analyzed with an X-ray fluorescence (XRF: Rigaku RIX-3000) at the National Institute of Polar Research. The analytical procedure followed the methods of Motoyoshi and Shiraishi (1995) and Motoyoshi *et al.* (1996). Modal mineral compositions were determined with the standard point counting method on thin sections. Bulk densities were determined using a pycnometer. The results are given in Table 1.

Table 1. Representative whole rock compositions analyses of major and trace elements, modal percentages of major minerals and density for rocks from Lützow-Holm Complex.

Sample name	92010905A	SN-119-02B	RK-131-05	BC-3	93012413D	BC-1	BC-2	93011801	SN-120-11
Rock type	clino pyroxenite	2Px-amphibolite	Px-Hb gneiss	Hb gneiss	calc-silicate gneiss	felsic gneiss	felsic gneiss	Bt-Opx-hb granulite	Bt-2Px granulite
Locality	Rundvag-shetta	Strandnibba	Rundvags-kollane	Ongle Is	Austhovde	Ongle Is	Ongle Is	Berrodden	Strandnibba
Major elements (wt%) *									
SiO_2	51.39	47.67	44.81	49.71	69.14	81.34	71.53	45.13	51.32
TiO_2	0.18	1.11	1.70	0.78	0.26	0.29	0.26	2.20	0.57
Al_2O_3	3.43	10.93	17.61	21.87	14.84	8.27	11.03	17.15	11.70
Fe_2O_3	7.06	12.42	14.58	6.10	1.30	1.47	2.41	15.36	10.04
MnO	0.14	0.15	0.16	0.05	0.03	0.02	0.05	0.24	0.16
MgO	15.56	13.31	5.38	3.28	1.46	0.31	1.11	5.54	10.11
CaO	17.25	8.47	9.01	9.55	7.34	0.65	2.39	7.70	9.44
Na_2O	0.63	2.00	2.31	4.13	3.13	1.19	1.44	1.84	2.32
K_2O	1.12	2.06	0.82	1.21	0.55	4.53	6.32	1.96	2.73
P_2O_5	0.01	0.12	0.21	0.02	0.26	0.00	0.09	0.28	0.30
total	96.77	98.24	96.59	96.69	98.31	98.06	96.63	97.41	98.68
Trace elements (ppm)*									
Ba	187.8	450.5	99.9	226.8	242.4	863.4	948.6	677.2	552.1
Co	65.0	83.9	60.0	15.9	2.1	1.8	2.7	43.3	53.9
Cr	2829.0	1176.0	28.7	26.8	8.7	12.5	29.6	33.2	1063.7
Cu	0.0	30.7	52.0	21.1	2.0	0.0	2.5	2.7	9.4
Nb	3.3	5.5	4.1	5.9	8.3	6.9	6.7	5.7	2.6
Ni	255.4	823.2	42.7	10.8	0.0	0.0	6.4	31.8	183.9
Rb	85.0	75.9	15.2	16.6	20.2	154.3	224.9	70.1	129.0
Sr	29.5	185.3	415.4	1149.4	936.6	204.3	805.0	198.1	369.3
V	98.5	255.5	377.8	97.0	17.8	17.6	45.8	126.7	201.3
Y	21.3	20.8	14.0	19.8	23.7	3.7	27.4	28.8	16.1
Zn	71.2	95.9	142.0	99.9	11.2	26.2	44.5	160.5	86.3
Zr	30.2	77.8	57.6	72.8	80.0	134.4	203.1	122.7	57.1
Modal percentage (vol%)									
quartz	0.0	0.0	0.0	0.0	44.6	42.6	59.6	0.0	0.0
K-feldspar	0.0	0.0	0.0	0.0	0.0	52.0	35.0	0.0	0.0
plagioclase	0.0	11.6	46.6	62.3	31.0	3.1	3.6	45.6	33.3
hornblende	1.3	70.6	25.8	34.3	0.0	0.0	0.0	10.0	3.6
orthopyroxene	27.3	0.3	7.4	0.0	0.0	0.0	0.0	19.6	3.6
clinopyroxene	60.6	1.6	10.2	0.0	21.0	2.0	0.6	0.0	26.6
biotite	10.6	15.6	8.4	2.6	0.0	0.3	0.6	22.6	31.0
sphene	0.0	0.0	0.0	0.0	3.3	0.0	0.0	0.0	0.0
opaque	0.0	0.0	1.6	0.0	0.0	0.0	0.0	0.0	1.0
grain size (mm)	0.1-0.5	0.1-0.5	0.2-0.5	0.5-1.5	0.5-2.0	0.5-2.0	0.1-1.0	0.1-1.0	0.2-0.5
density (g/cm³)	3.35	3.19	3.11	2.96	2.88	2.79	2.73	3.13	3.07

BC; Bored core of JARE 22 in Ongle islands. 1: depth=450 cm, 2: depth=1375cm, 3: depth=1500cm
*: XRF analyses

2.1. Clinopyroxenite (Sp. No. 92010905A)

This rock was collected from Rundvågshetta, Soya Coast (Motoyoshi *et al.*, 1986). The rock consists mainly of fine-grained clinopyroxene and orthopyroxene (over 85 mod%; Table 1) with minor biotite and poikiloblastic hornblende. Apatite occurs as an accessory mineral (Fig. 2a). Biotite flakes are aligned to define foliation.

2.2. Two-pyroxene amphibolite (Sp. No. SN-119-02B)

Two-pyroxene amphibolite (hereafter, 2Px-amphibolite) was collected from Strandnibba, Sôya Coast (Motoyoshi *et al.*, 1985). The rock is predominantly composed of medium-grained hornblende, biotite, plagioclase and minor amounts of fine-grained and equigranular clinopyroxene and orthopyroxene (Fig. 2b). The rock exhibits lineation defined by aligned biotite flakes. Accessory minerals are apatite and ilmenite.

2.3. Pyroxene-hornblende gneiss (Sp. No. RK-131-05)

Pyroxene-hornblende gneiss (hereafter, Px-Hb gneiss; Fig. 2c) from Rundvågskollane, Sôya Coast (Motoyoshi *et al.*, 1986) contains predominant amounts of medium-grained plagioclase, hornblende, clinopyroxene and poikiloblastic orthopyroxene. The plagioclase shows remarkable zonal structure. The rock exhibits weak gneissosity defined by aligned hornblende, orthopyroxene and clinopyroxene grains.

2.4. Hornblende gneiss (Sp. No. BC-3)

Hornblende gneiss (hereafter, Hb-gneiss; Fig. 2d) is a core sample (surface level) recovered from 1500-cm core-drilling at the Syowa Station area. The rock shows a layering structure characteristic of the hornblende-rich and plagioclase-rich layer. The constituent minerals are poikiloblastic and brown hornblende and plagioclase. Accessory minerals are apatite and ilmenite.

2.5. Calc-silicate gneiss (Sp. No. 93012413D)

This rock was collected from Austhovde, Sôya Coast (Shiraishi and Yoshida, 1987). The gneiss (Fig. 2g) is a medium-grained rock and consists of quartz, plagioclase and clinopyroxene. Accessory minerals are rounded to oval-shaped sphene and ilmenite. Quartz shows wavy extinction and has some aligned fluid and sphene inclusions. Weakly elongated clinopyroxene grains define gneissosity.

2.6. Felsic gneisses (Sp. No. BC-1, BC-2)

The felsic gneisses are from drilling cores at the Syowa Station surface. They were recovered from cores at surface depths of 450-cm (Sp. No. BC-1) and 1375-cm (Sp. No. BC-2), respectively. Felsic gneiss (BC-1) is a fine-grained rock, mainly composed of quartz and K-feldspar with a minor amount of biotite. Zircon and fine-grained biotite are additional minor mineral constituents. Some biotite grains show pseudomorph after orthopyroxene. The felsic gneiss (BC-2) is a medium-grained rock with the porphyroblastic texture. The rock is composed of quartz and mesoperthite with a minor amount of zircon.

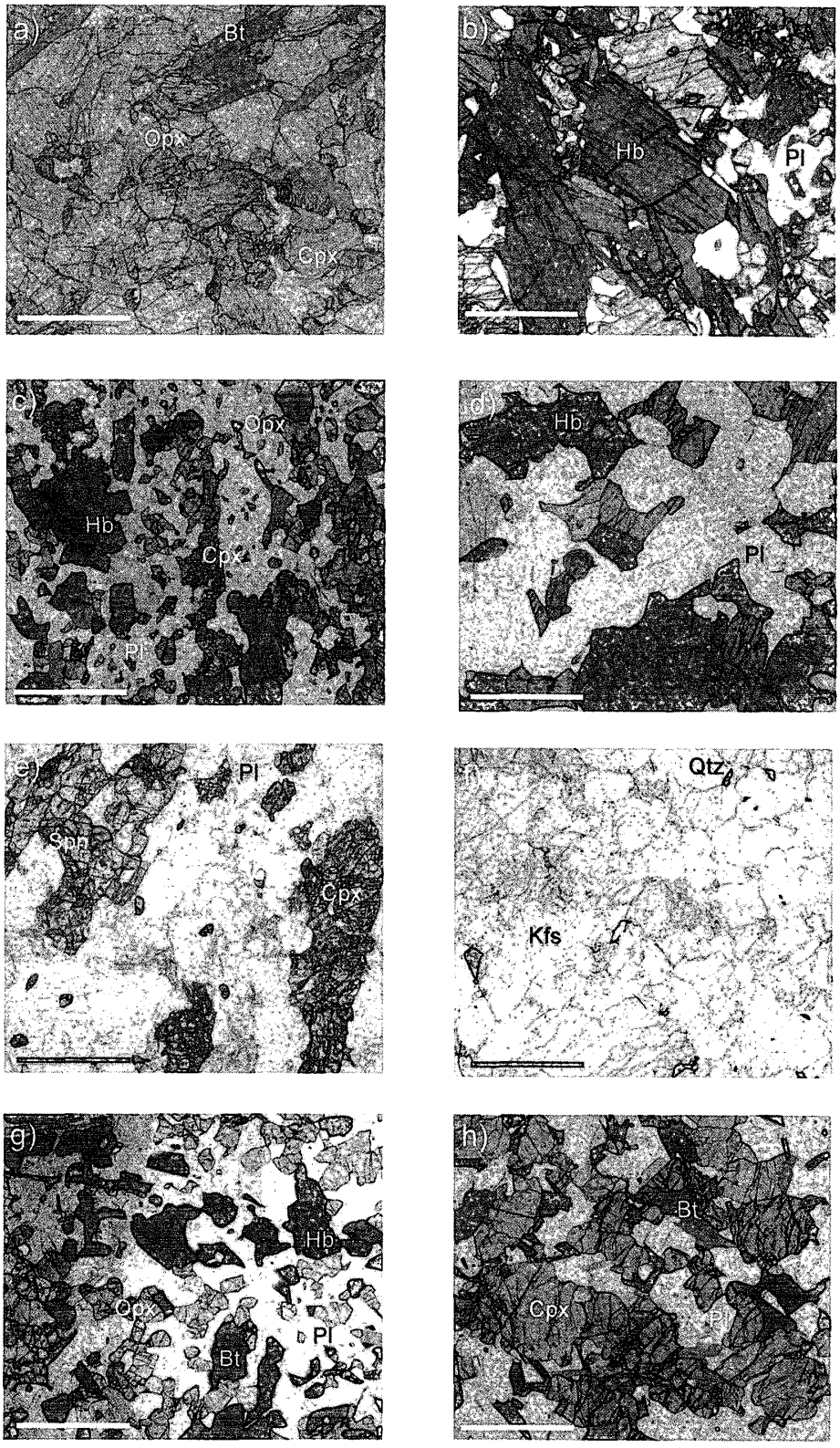

Fig. 2. Photomicrographs of representative metamorphic rocks in the Lützow-Holm Complex. Scale bars are 1.0 mm. a) clinopyroxenite. b) 2PX-amphibolite. c) Px-Hb gneiss. d) Hb gneiss. e) Bt-Opx-Hb granulite. f) Bt-2Px gneiss. g) calc-silicate granulite. h) felsic gneiss.

2.7. Biotite-orthopyroxene-hornblende granulite (Sp. No. 93011801)

This is a dike rock collected from Berrodden, Sôya Coast. The rock is medium-grained granulite showing porphyroblastic texture. It consists of biotite, plagioclase, orthopyroxene and brown hornblende. Accessory minerals are zircon and ilmenite. The biotite flakes make a weak foliation.

2.8. Biotite-two pyroxene granulite (Sp. No. SN-120-11)

This rock was collected from Strandnibba, Sôya Coast (Motoyoshi *et al.*, 1985). The sample is medium-grained rock with nearly equal amounts of biotite, plagioclase and pyroxenes. Accessory minerals are ilmenite and apatite. This rock shows the porphyroblastic texture.

3. Experimental technique

P-wave velocities in the rock samples were measured up to 1.0 GPa in a temperature range from 15 to 400°C with a piston-cylinder apparatus (34-mm borehole) at the Geological Institute, Yokohama National University, Japan. The rock samples were cut in 14 mm diameter and 12 mm long up both ends were polished. The sample-cores were oven-dried (at 110°C and for 24 hours) to minimize the effect of pore fluid on velocity measurements. $LiNbO_3$ piezoelectric transducers were mounted on both ends of the sample core (Fig. 3). The Pt-Rh_{13} thermocouple for temperature measurements was placed at the top of the sample. The temperature difference between the center and top end of the sample-core is less than 2°C at 400°C. The sample-core with transducers and talc rods was set in a carbon heater (Fig. 3). Measurements of velocity were carried out using the pulse transmission technique, which consists of determination of travel time of an ultrasonic wave through a sample-core of known length (Birch, 1960). All pulses were

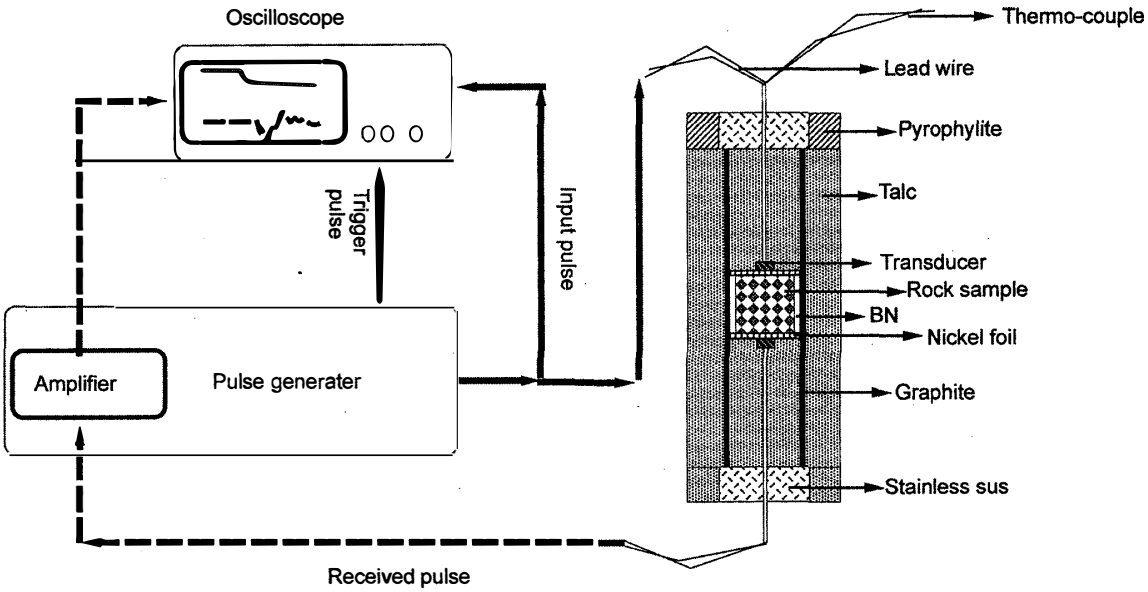

Fig. 3. Schematic diagram of the cell assembly for P-wave velocity measurement and of the electrical equipment.

4096 time-stacked to reduce the effect of electric noise. The delay time (travel time through the sell system) was measured using a special cell assembly, which is directly contacted both transducers without a rock sample. Electric pulses were recorded using a digital oscilloscope which sampling rate of 2.0×10^{10} Sa/s. Errors in ultrasonic velocity measurements are less than 0.03 km/s. The main sources of errors are inaccuracy of core length measurement and travel time determination. The velocities reported here were not corrected for length changes during compression. The shortening of specimen length is estimated to be approximately 1.65×10^{-9} mm at 1.0 GPa based on theoretical calculation from the bulk modulus of single minerals (Anderson *et al.*, 1968; Birch, 1961; Ryzhova and Alexsandrov, 1965; Simmons and Wang, 1971). The estimated length-change is equivalent to about 1.30×10^{-7} km/s in *P*-wave velocity. Previous studies reported that foliated rocks have significant velocity anisotropy (*e.g.* Kern *et al.*, 1997). In this study, we measured rock velocities of foliated rocks in the direction parallel to both foliation and lineation.

4. Results and discussion

4.1. P-wave velocity vs. pressure

To examine the pressure effect on *Vp*, *Vp* values were measured in a pressure range of 0.1 to 1.0 GPa at 25°C for five rock samples: clinopyroxenite, felsic gneiss (BC-1), Px-Hb gneiss, 2Px-amphibolite and Bt-2Px granulite. *Vp* values measured during pressurization (from 0.1 to 1.0 GPa) are shown in Fig. 4 together with those measured during depressurization (from 1.0 to 0.1 GPa). During pressurization, *Vp* increases non-linearly at relatively lower pressure conditions (below about 0.5 GPa) and then it is nearly constant or slightly increases at higher pressure up to 1.0 GPa. The *Vp* values obtained below 0.6 GPa during decompression are much higher than those obtained during pressurization. The *Vp*-hysteresis is interpreted as being due to unopened micro-cracks, which were once closed during pressurization at higher 1.0 GPa (Birch, 1960; Christensen, 1965). Previous studies have reported that the *Vp*-hysteresis is commonly noted at pressure below 0.2 GPa (*e.g.*, Christensen, 1965). However, in this study the upper pressure limit of the *Vp*-hysteresis was around 0.6 GPa in most rocks studied (Fig. 4b, c, d and f) and 0.9 GPa in the two-pyroxene amphibolite (Fig. 4e). The *Vp*-hysteresis parameter of the measured rocks, which is defined by a percentage of *Vp* difference from the average *Vp* at a given pressure, ranges from 0.0 to 0.8% at 0.6 GPa and from 0.5 to 6.6% at 0.4 GPa. The difference of *Vp*-hysteresis between each sample can be explained by differences in volume percentage and shape of both microcracks and pores (Walsh, 1965).

4.2. P-wave velocity vs. temperature

The thermal effect on *Vp* was examined in the temperature range from 25 to 400°C at 0.4, 0.6 and 1.0 GPa during pressurization for the felsic gneisses (BC-1 and BC-2) and the Bt-2Px granulite (SN-120-11). *Vp* values were also measured for the clinopyroxenite (92010905A) from 25 to 400°C at 1.0 GPa (Fig. 5). With increasing temperature at 0.4 GPa, *Vp* values of the felsic gneisses and the Bt-2Px gneiss slightly decrease up to 200°C, then show a rapid decrease at high temperature above 200°C (Fig. 5a). Figure 5b

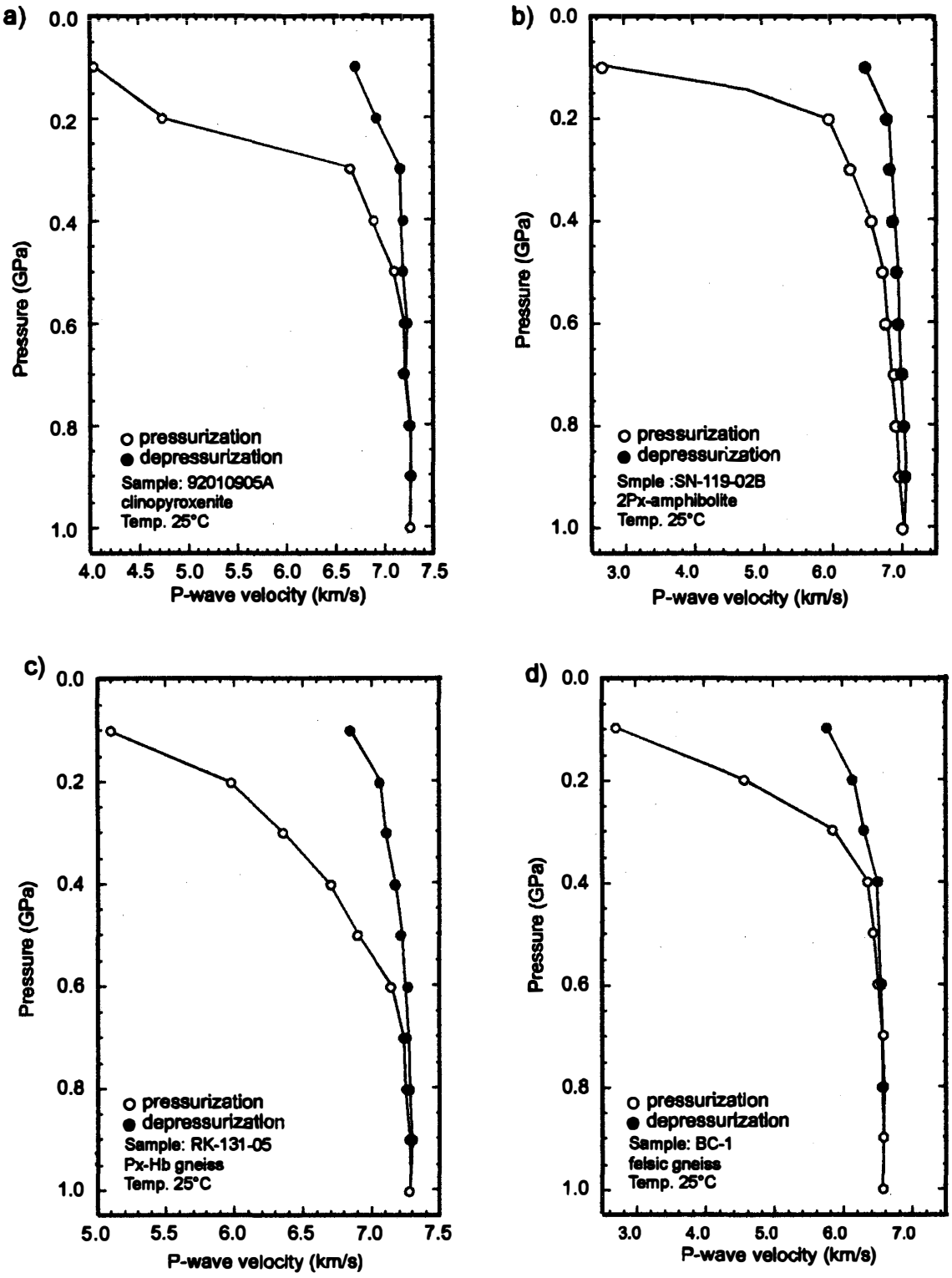

Fig. 4. a) Vp vs. pressure curves of Lützow-Holm Complex rocks. Pressurizing upward atmospheric pressure to 1 GPa. Temperature: 25°C. b) Vp hysteresis of clinopyroxenite in pressure at 25°C. Open circle: pressurizing up to 1.0 GPa, close circle: depressurizing down to 0.1 GPa. c) Vp hysteresis of felsic gneiss. d) Vp hysteresis of Px-Hb gneiss. e) Vp hysteresis of 2Px-amphibolite. f) Vp hysteresis of Bt-2Px granulite.

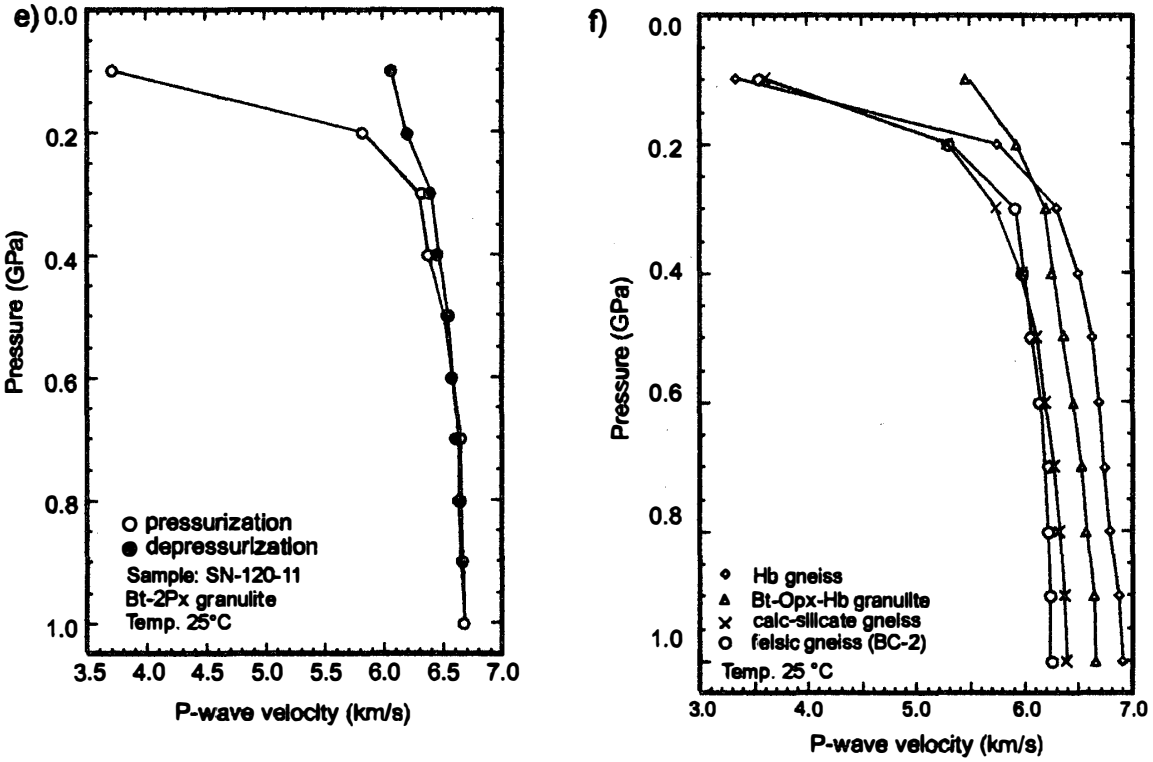

Fig. 4 (continued).

show *Vp* of the felsic gneisses and the Bt-2Px granulite at 0.6 GPa. Only a small drop of *Vp* (0.04–0.03 km/s) was observed for the felsic gneisses during heating. In contrast, *Vp* of the Bt-2Px granulite decreases rapidly from 6.59 km/s at 200°C to 6.06 km/s at 400°C. At 1.0 GPa, *Vp* values of the clinopyroxenite and the felsic gneisses show slightly lower *Vp* values at higher temperatures, while the Bt-2Px granulite exhibits a relatively strong negative thermal effect on *Vp*, which drops from 6.68 km/s at 25°C to 6.24 km/s at 400°C (Fig. 5c).

All of the rocks measured show relatively large thermal effect on *Vp* at lower pressure conditions (0.4 GPa). This is probably due to both thermal cracking (Kern and Richter, 1981) and change of elastic properties of mineral constituents. The change of *Vp* at high pressures above 0.6 GPa is mainly due to the thermal effect on the elastic properties of crystals (*cf.* Kern *et al.*, 1997). This could be explained by weakening of interatomic bonds in crystal structure with heating. The elastic properties of crystals highly depend on the strength of interatomic bonds in the crystal structure (Alexandrov and Ryzhova, 1961). The Bt-2Px granulite shows the most remarkable velocity drop of 0.45 km/s between 25°C and 400°C at 1.0 GPa. In the case of the Bt-2Px granulite, biotite, which is the most dominant mineral constituent, would primarily contribute the velocity drop, because interatomic bonds in the crystal structure of biotite are weaker than those of other mineral constituents such as pyroxene, plagioclase and hornblende (Alexandrov and Ryzhova, 1961).

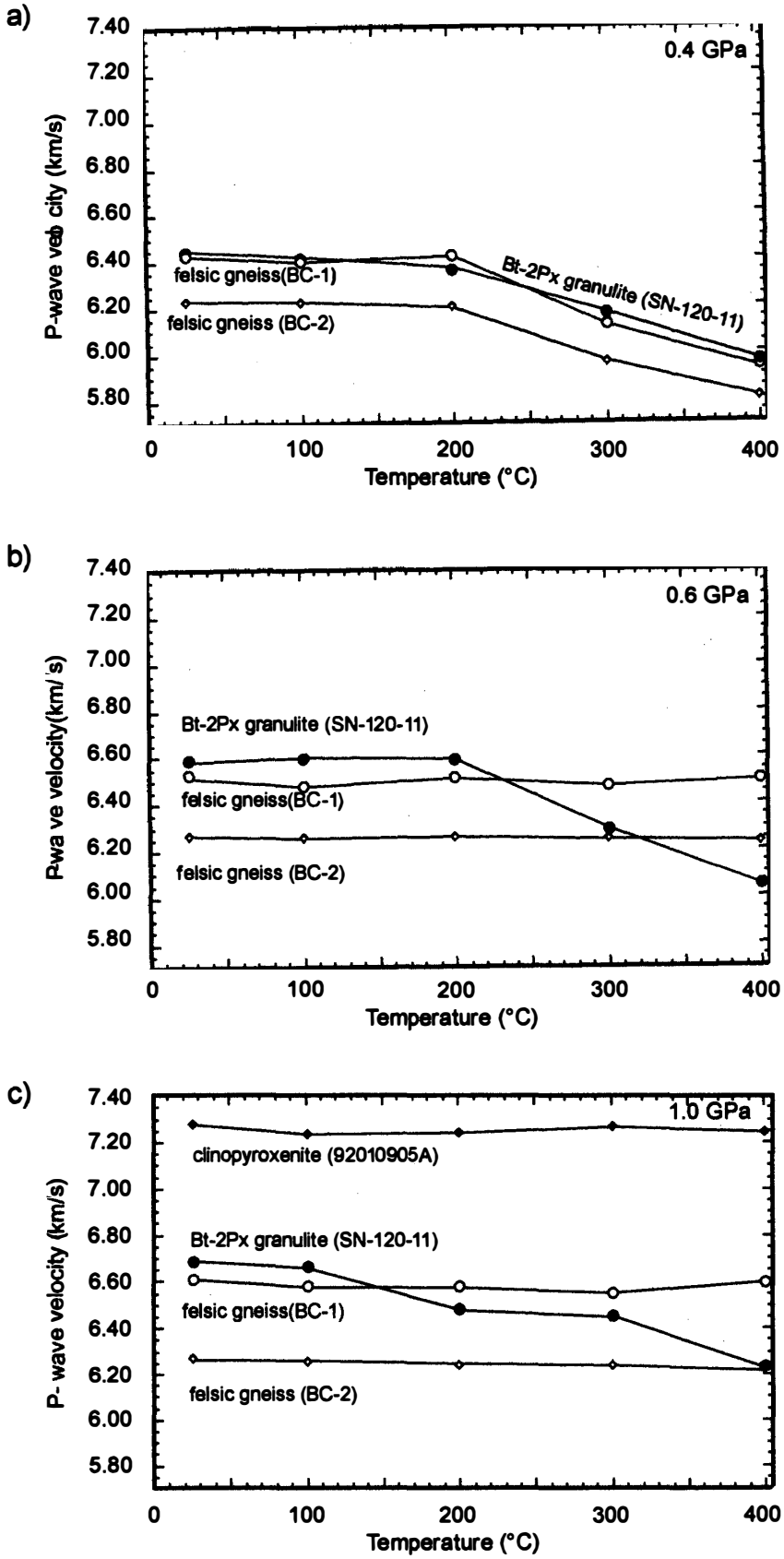

Fig. 5. Relationship between velocity and temperature for the granulite from the Lützow-Holm Complex in the temperature range between 25°C and 400°C, a) at 0.4 GPa, b) at 0.6 GPa, c) at 1.0 GPa.

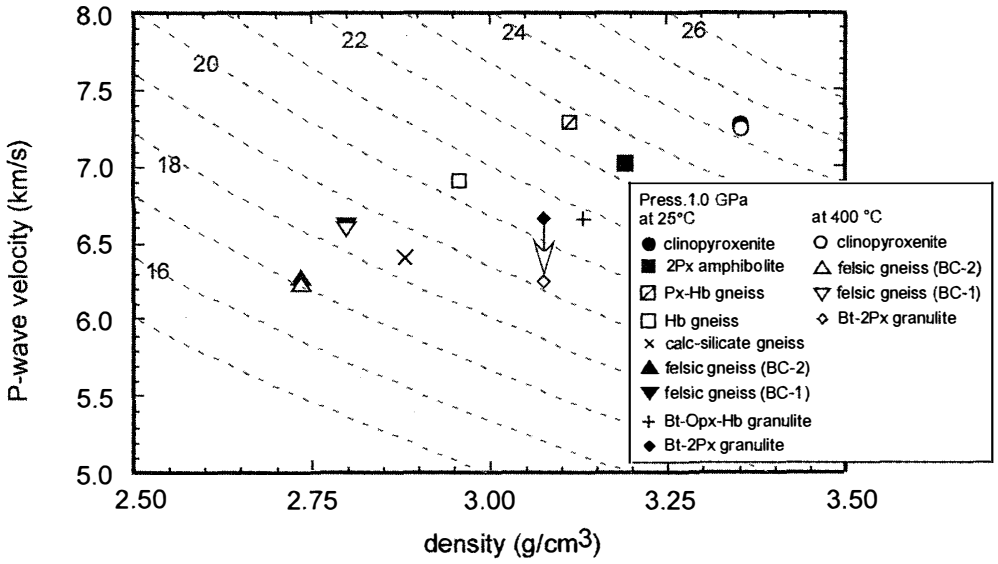

Fig. 6. P-wave velocity (determined at 1.0 GPa and 25°C) versus density diagram with curves of constant acoustic impedance ($\times 10^6$ kg/m^2 s).

Table 2. P-wave velocities (Vp) at various confining pressure and temperature.

Press.	Temp.	clino-pyroxenite	2Px-amphibolite	Px-Hb gneiss	Hb gneiss	calc-silicate gneiss	felsic gneiss (BC-1)	felsic gneiss (BC-2)	Bt-Opx-Hb granulite	Bt-2Px granulite
Pressurizing										
0.1 GPa	25°C	4.044	2.683	5.117	3.321	3.610	2.723	3.558	5.448	3.721
0.2 GPa		4.741	5.975	5.991	5.738	5.277	4.578	5.312	5.917	5.823
0.3 GPa		6.664	6.285	6.364	6.304	5.752	5.865	5.920	6.208	6.332
0.4 GPa		6.897	6.580	6.720	6.500	5.994	6.401	5.994	6.253	6.391
0.5 GPa		7.113	6.754	6.905	6.629	6.116	6.428	6.077	6.334	6.539
0.6 GPa		7.241	6.797	7.157	6.695	6.198	6.526	6.158	6.495	6.583
0.7 GPa		7.197	6.905	7.242	6.705	6.284	6.600	6.240	6.523	6.660
0.8 GPa		7.253	6.983	7.269	6.737	6.340	6.590	6.234	6.536	6.639
0.9 GPa		7.293	7.001	7.284	6.873	6.385	6.607	6.253	6.637	6.671
1.0 GPa		7.279	7.027	7.288	6.910	6.404	6.608	6.269	5.786	6.684
Depressurizing										
0.9 GPa	25°C	7.270	7.064	7.308	nd	nd	6.608	nd	nd	6.670
0.8 GPa		7.270	6.962	7.288	nd	nd	6.581	nd	nd	6.660
0.7 GPa		7.212	6.963	7.269	nd	nd	nd	nd	nd	6.622
0.6GPa		7.212	6.968	7.278	nd	nd	6.508	6.264	nd	6.583
0.5GPa		7.204	6.946	7.223	nd	nd	nd	nd	nd	6.399
0.4 GPa		7.198	6.890	7.181	nd	nd	6.438	6.230	nd	6.421
0.3 GPa		7.177	6.839	7.123	nd	nd	6.323	nd	nd	6.404
0.2 GPa		6.827	6.801	7.069	nd	nd	6.161	nd	nd	6.179
0.1 GPa		6.715	6.499	6.854	nd	nd	5.786	nd	nd	6.074
1.0 GPa	100°C	7.236	nd	nd	nd	nd	6.580	6.257	nd	6.665
	200°C	7.243	nd	nd	nd	nd	6.585	6.244	nd	6.483
	300°C	7.270	nd	nd	nd	nd	6.556	6.245	nd	6.455
	400°C	7.250	nd	nd	nd	nd	6.604	6.231	nd	6.240
0.6 GPa	100°C	nd	nd	nd	nd	nd	6.480	6.254	nd	6.597
	200°C	nd	nd	nd	nd	nd	6.511	6.253	nd	6.586
	300°C	nd	nd	nd	nd	nd	6.481	6.249	nd	6.293
	400°C	nd	nd	nd	nd	nd	6.506	6.233	nd	6.055
0.4 GPa	100°C	nd	nd	nd	nd	nd	6.400	6.223	nd	6.404
	200°C	nd	nd	nd	nd	nd	6.421	6.200	nd	6.358
	300°C	nd	nd	nd	nd	nd	6.124	5.956	nd	6.171
	400°C	nd	nd	nd	nd	nd	5.941	5.807	nd	5.964
Acoustic impedance										
1.0 GPa	25°C	24.4	23.6	21.0	19.9	20.0	18.5	17.1	17.1	20.8
	400°C	24.3	nd	nd	nd	nd	18.5	17.0	nd	19.4

nd: no data

4.3. P-wave velocity vs. density

The present data indicate a positive correlation between *Vp* and rock density (Fig. 6). This result is consistent with previous studies (*e.g.*, Birch, 1961). Intensities of acoustic impedance of the rock samples at 25°C and 1.0 GPa and at 400°C and 1.0 GPa were calculated from the present data (Table 2). Contours of constant acoustic impedance ($\times 10^6$ kg/m^{2}s) are shown in Fig. 6. The contrast of acoustic impedance appears as the reflectors (Hurich *et al.*, 2001). There is a large contrast between the felsic gneisses and Bt-2px granulite at 25°C and 1.0 GPa. However, this contrast becomes obscure at 400°C and 1.0 GPa (Fig. 6). The Bt-2px granulite shows a significant drop of acoustic

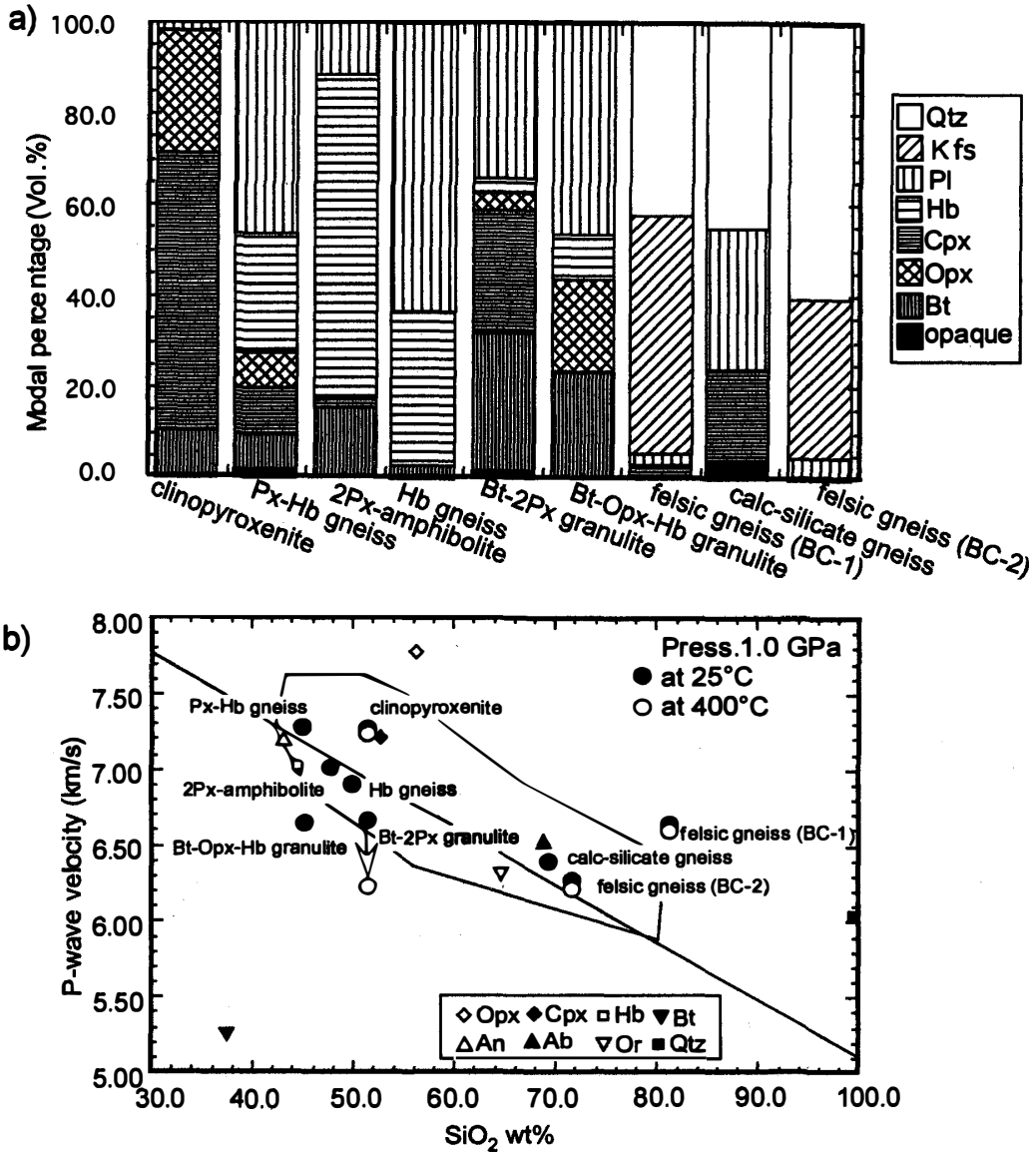

Fig. 7. a) Modal percentage of main constituent minerals. b) Relationship between SiO_2 wt% vs. Vp. Vp values of constituent minerals at 1.0 GPa are also shown (Anderson et al., 1968; Birch, 1961; Ryzhova and Aleksandrov, 1965; Simmons and Wang, 1971). Line: $Vp=8.91-0.28\times SiO_2$ wt% is after Rudnick and Fountain (1995). Ab: albite, An: anorthite, Bt: biotite, Cpx: clinopyroxene, Hb: hornblende, Kfs: alkali feldspar, Opx: orthopyroxene, Or: orthoclase, Pl: plagioclase, Qtz: quartz.

impedance with the rise of temperature from 25°C to 400°C (Table. 2).

4.4. Relationship between Vp and lithology

Relationship between *Vp* and mineral assemblage was examined for the six rock samples with ultra-basic to basic composition. *Vp* values measured at 25°C exhibit negative correlation with SiO_2 content in the range of SiO_2 45–82 wt% (Fig. 7b). Previous studies reported a similar relationship between *Vp* and SiO_2 content (*e.g.*, Rudnick and Fountain, 1995). The clinopyroxenite and Px-Hb gneiss have high *Vp* values (*Vp*=7.28, 7.29 km/s) that may be due to the relatively high abundance of orthopyroxene. The Bt-Opx-Hb granulite and the Bt-2Px granulite, which are characterized by high abundance of biotite (22.6 and 31.0 vol%), show relatively lower *Vp* (about 0.5 km/s) than other basic granulites with comparable SiO_2. At 400°C, *Vp* values in the basic rocks, except for *Vp* in the biotite-bearing rocks, also show negative correlation with SiO_2 content in the rocks (Fig. 7). This *Vp*-SiO_2 correlation is well represented by the combination of modal proportions and single crystal velocities of constituent minerals including orthopyroxene, clinopyroxene, hornblende, quartz, and feldspar (albite, anorthite, and orthoclase) (Fig. 7). Higher abundance of biotite may significantly lower *Vp* in middle to lower crustal rocks with basic composition.

5. Summary

This study gives a new data set of *P*-wave velocity for nine granulite facies metamorphic rocks of the Lützow-Holm Complex, East Antarctica. These samples have a wide range of SiO_2 content from ultra-basic to acidic composition (44.8–81.3 wt%) The main conclusions of this study are summarized as follow:

1) During pressurization, *Vp* increases non-linearly at relatively lower pressure conditions (below about 0.5 GPa) and then it is nearly constant or slightly increases at higher pressure up to 1.0 GPa. The *Vp* values obtained below 0.6 GPa during decompression are much higher than those obtained during pressurization. Although previous studies have reported that *Vp*-hysteresis was usually detected at pressure below 0.2 GPa (*ex.* Christensen, 1965), the present study indicates that the upper pressure limit of the *Vp*-hysteresis is at around 0.6 GPa in most rocks studied and 0.9 GPa in the two-pyroxene amphibolite. The *Vp*-hysteresis parameter of the measured rocks ranges from 0.0 to 0.8% at 0.6 GPa and from 0.5 to 6.6% at 0.4 GPa.

2) The thermal effect on *Vp* was examined in the temperature range from 25 to 400°C at 0.4, 0.6 and 1.0 GPa during pressurization for the felsic gneisses and mafic granulites. The Bt-2Px granulite shows the most remarkable velocity drop of 0.45 km/s between 25°C and 400°C at 1.0 GPa, suggesting that biotite, which is the dominant mineral constituent in this rock, would primarily contribute this velocity drop.

3) At 1.0 GPa and 400°C, the biotite-bearing mafic granulite shows relatively low *Vp*, which is equivalent to that of the felsic gneiss. The biotite-bearing rock is characterized by relatively lower acoustic impedance than the biotite-free mafic granulite at a given SiO_2 content.

Acknowledgments

We thank Dr. Y. Motoyoshi (NIPR) for providing most of the rock samples. K.K. also thanks Drs. Y. Nogi, M. Kanao, S. Baba, T. Hokada (NIPR) and A. Kubo (National Institute for Earth Science and Disaster Prevention) for their constructive discussion and encouragement. This study was supported by a Grant-in-Aid for Scientific Research from the Japanese Society for the Promotion of Science to M.A. (10440151 and 12440147)

References

Alexandrov, S.K. and Ryzhova, V.T. (1961): The elastic properties of rock forming minerals, II, Layered silicates. Bull. Acad. Sci. USSR, Geophys. Ser. Engl. Transl., **9**, 1165–1168.

Anderson, O.L., Schreiber, E., Liebermann, R.C. and Soga, N. (1968): Some elastic constant data on minerals relevant to geophysics. Rev. Geophys., **6**, 491–524.

Birch, F. (1960): The velocity of compressional wave in rocks to 10 kilobars, Part 1. J. Geophys. Res., **65**, 1083–1102.

Birch, F. (1961): The velocity of compressional wave in rocks to 10 kilobars, Part 2. J. Geophys. Res., **66**, 2199–2224.

Blundell, D., Freeman, R. and Mueller, S. (1992): A Continent Revealed. The European Geotraverse. Cambridge, Cambridge Univ. Press, 273 p.

Condie, C.K. (1997): Plate Tectonics and Crustal Evolution. 4th ed. Oxford, Butterworth-Heinmann, 282 p.

Christensen, I.N. (1965): Compressional wave velocities in metamorphic rocks at pressures to 10 kilobars. J. Geophys. Res., **70**, 6147–6164.

Hiroi, Y., Shiraishi, K. and Motoyoshi, Y. (1991): Late Proterozoic paired metamorphic complexes in East Antarctica, with special reference to the tectonic significance of ultramafic rocks. Geological Evolution of Antarctica, ed. by M.R.A. Thomson *et al.* Cambridge, Cambridge Univ. Press, 83–87.

Hurich, A.C., Deemer, J.S. and Indares, A. (2001): Compositional and metamorphic controls on velocity and reflectivity in the continental crust: An example from the Grenville Province of eastern Quebec. J. Geophys. Res., **106**, 665–682.

Ikami, A., Ito, K., Shibuya, K. and Kaminuma, K. (1984): Deep crustal structure along the profile between Syowa and Mizuho stations, East Antarctica. Mem. Natl Inst. Polar Res., Ser. C (Earth Sci.), **15**, 19–28.

Kern, H. and Richter, A. (1981): Temperature derivatives of compressional and shear wave velocities in crustal and mantle rocks at 6 kbar confining pressure. J. Geophys., **49**, 47–56.

Kern, H., Liu, B. and Popp, T. (1997): Relationship between anisotropy of *P* and *S* wave velocities and anisotropy of attenuation in serpentinite and amphibolite. J. Geophys. Res., **102**, 3051–3065.

Miyamachi, H., Murakami, H., Tsutsui, T., Toda, S., Minta, T. and Yanagisawa, M. (2001): A seismic refraction experiment in 2000 on the Mizuho Plateau, East Antarctica (JARE-41)—Outline and observations. Nankyoku Shiryô (Antarct. Rec.), **45**, 101–147 (in Japanese with English abstract).

Motoyoshi, Y. and Ishikawa, M. (1997): Metamorphic and structural evolution of granulites from Rendvåshetta, Lützow-Holm Bay, East Antarctica. The Antarctic Region: Geological Evolution and Processes, ed. by C. A. Ricci. Siena, Terra Antarct. Publ., 65–72.

Motoyoshi, Y. and Shiraishi, K. (1995): Quantitative chemical analysis of rocks with X-ray fluorescence analyzer: (1) Major elements. Nankyoku Shiryô (Antarct. Rec.), **39**, 40–48 (in Japanese with English abstract).

Motoyoshi, Y., Matsubara, S., Matsumoto, Y., Moriwaki, K., Yanai, K. and Yoshida, Y. (1985): Explanatory text of geological map of Strandnibba, Antarctica. Antarct. Geol. Map Ser., Sheet 26. Tokyo, Natl Inst. Polar Res., 10 p. with 8 pl.

Motoyoshi, Y., Matsueda, H., Matsubara, S., Moriwaki, K., Sasaki, K. and Moriwaki, K. (1986):

Explanatory text of geological map of Rundvågskollane and Rundvågshetta, Antarctica. Antarct. Geol. Map Ser., Sheet 24. Tokyo, Natl Inst. Polar Res., 11 p. with 14 pl.

Motoyoshi, Y., Ishizuka, H. and Shiraishi, K. (1996): Quantitative chemical analysis of rocks with X-ray fluorescence analyzer: (2) Trace elements. Nankyoku Shiryô (Antarct. Rec.), **40**, 53–63 (in Japanese with English abstract).

Rudnick, L.R. and Fountain, M.D. (1995): Nature and composition of the continental crust: A lower crustal perspective. Rev. Geophys., **33**, 267–309.

Ryzhova, V.T. and Alexsandrov, S.K. (1965): The elastic properties of potassium-sodium feldspars. Izv., Acad. Sci., USSR, Phys. Solid Earth Ser., **1**, 98–102.

Shiraishi, K, and Yoshida, M. (1987): Explanatory text of geological map of Botnneset, Antarctica. Antarct. Geol. Map Ser., Sheet 25. Tokyo, Natl Inst. Polar Res., 9 p. with 8 pl.

Shiraishi, K., Ellis, J.D., Hiroi, Y., Fanning, M.C., Motoyoshi, Y. and Nakai, Y. (1994): Cambrian orogenic belt in East Antarctica and Sri Lanka: Implications for Gondwana Assembly. J. Geol., **102**, 47–65.

Simmons, G. and Wang, H. (1971): Single Crystal Constants and Calculated Aggregate Properties: A Handbook. 2nd ed. Cambridge, MIT Press, 370 p.

Walsh, B.J. (1965): The effect of cracks on the compressibility of rock. J. Geophys. Res., **70**, 381–389.

(Received May 11, 2001; Revised manuscript accepted May 25, 2001)